Electrochemical Study of Haematoxylin Inhibitory Activity to Control Carbon Steel Corrosion in Natrium Nitrate Solution

Adriana Samide[*], *Bogdan Tutunaru, Cătălina Ionescu, Cristian Tigae, Anca Moanţă*

University of Craiova, Faculty of Sciences, Department of Chemistry, Calea Bucuresti 107 i, Craiova, Romania
[*]E-mail: samide_adriana@yahoo.com

The corrosion inhibition of carbon steel in 0.1 M NaNO$_3$ solution using haematoxylin (HX), IUPAC name 7,11b-Dihydroindeno[2,1-*c*]chromene-3,4,6a,9,10(6*H*)-pentol was studied using electrochemical measurements such as: potentiodynamic polarization and electrochemical impedance spectroscopy (EIS) in association with UV-Vis spectrophotometry. Microscopic images were used to examine the surface morphology. Electrochemical results showed that, for 1.0 mM HX in natrium nitrate solution, the corrosion current density (i_{corr}) had the lowest value (11.5 μA cm^{-2}), and the highest polarization resistance (R_p) was obtained (498.6 Ω cm^2), and consequently, an inhibition efficiency (*IE*) of 81.6±2% for HX was reached. A synergic action mechanism of HX was proposed related to the organic film formation consisting in haematoxylin and its oxidized form haematein (HT) adsorption, supplemented by evidence of HT complexes with Fe^{3+}, and an additional process of HX electropolymerization. By optical microscopy, the feature of the uniform layer on the surface was nuanced for carbon steel corroded in 0.1 M NaNO$_3$ solution containing 1.0 mM HX.

Keywords: corrosion inhibition; haematoxylin; electrochemical measurements; action mechanism; surface morphology

1. INTRODUCTION

The destruction of iron and iron alloys by chemical and electrochemical reactions with their environment is a major industrial problem that has attracted researchers' interest. Hydrochloric and sulphuric acids are widely used for pickling or cleaning in industrial applications and because of their highly corrosive nature they may cause serious problems.

A useful method, among others, to protect steels and iron in aggressive acidic environments, is the addition of inhibitors in the solutions with which the metals come into contact, in order to inhibit the corrosion reactions and to reduce the corrosion rate. Organic inhibitor molecules can physically or

chemically adsorb on metal surface and form a surface layer that protects the metal from corrosion. Inhibition efficiency is closely related to certain factors: the presence of functional groups, the presence of heteroatoms, lone electron pairs in the heteroatoms, molecular size, electron density, steric factor (i.e. planarity), π-electrons, conjugated bonds [1-9].

In the past years, many classes of organic compounds have been tested as inhibitors. Increased attention has been dedicated to eco-friendly corrosion inhibitors, which have been exploited as a green alternative to synthetic and toxic chemicals [10, 11].

These compounds include amino acids and their derivatives. Weight loss, potentiodynamic polarization, electrochemical impedance spectroscopy, AFM and EDX analyses have been used to study the corrosion inhibition of adenine and L-tryptophan [12, 13]. The application of anionic, cationic or gemini surfactants, have remarkable inhibition efficiency, near their critical micellar concentration [14-17].

Imidazolium, alkilimidazolium and some pyridinium- or vinyl- based ionic liquids have been tested as corrosion inhibitors for steel, using potentiodynamic polarization, linear polarization and weight loss methods. This type of compounds presents relatively high inhibition efficiencies (80-96 %) [18-20]. Monoethanolamine was used to convert polyethylene terephthalate waste into a water soluble amide as corrosion inhibitor for carbon steel in 1M HCl [21]. Few articles are reported on the corrosion inhibition of carbon steel with polymeric inhibitors: polyvinyl pyrrolidone, poly(ethylene glycol) methyl ether, polyacrylamide [22-24]. Organic dyes have been reported as effective corrosion inhibitors of carbon steel in acidic media. The inhibition effect of Methylene Blue, Methyl Red, New Fuchsin, Nile Blue, Indigo Carmine, Alizarin Yellow, Bromophenol Blue, Thymol Blue, Basic yellow 13, Basic yellow 28, has been studied [25-32].

The use of antibiotics and other drugs has been investigated and inhibition efficiencies are correlated with their heterocyclic structure. A theoretical study on the electronic and molecular structures of sulfaacetamide, sulfapyridine, sulfamerazine, and sulfathiazole was used to determine the relationship between some quantum chemical parameters and inhibition efficiencies [33]. The inhibitory properties of Penicillin G, Chloroquine, Cloxacillin and Trimethoprim have also been reported [34-37].

Several studies have been carried out on the inhibition of carbon steel corrosion by plant extracts of Asteriscus Graveolens [38], Jatropha curcas [39], Sesamum indicum [40], Phyllanthus Amarus [41] species.

Haematoxylin, IUPAC name: 7,11b-Dihydroindeno[2,1-*c*]chromene-3,4,6a,9,10(6*H*)-pentol, is a natural compound extracted from the heartwood of the Central American logwood Haematoxylon campechianum Linnaeus.

In this work, the inhibition activity of haematoxylin (HX) has been evaluated for carbon steel corrosion in 0.1 M NaNO$_3$ solution using electrochemical measurements associated with UV-Vis spectrophotometry.

2. MATERIALS AND METHODS

2.1. Materials

The used material was a carbon steel plate (20mm x 20mm x 2mm) with the following composition (weight %): C=0.1%; Si=0.035%; Mn=0.4%; Cr=0.3%; Ni=0.3%; Fe=the remainder. The samples were mechanically polished with emery paper, degreased with acetone and dried. Corrosion tests were performed in 0.1 M $NaNO_3$ blank solution and 0.1 M $NaNO_3$ containing different concentrations of haematoxylin: $4 \cdot 10^{-4}$ M, $6 \cdot 10^{-4}$ M, $8 \cdot 10^{-4}$ M and 10^{-3} M. All reagents were obtained from Merck.

2.2. Electrochemical measurements

Potentiodynamic polarization was used to determine the corrosion rate of carbon steel in the presence and in the absence of haematoxylin. All the electrochemical measurements were obtained using a VoltaLab 40 potentiostat/galvanostat, VoltaMaster 4 software, connected to a personal computer. A glass corrosion cell with a platinum counter electrode, a saturated $Ag/AgCl_{sat}$ reference electrode and carbon steel sample as working electrode were used. The immersion time of the plates in the respective media was of 4 minutes in open circuit, at room temperature. The polarization curves were registered with a scan rate of 1 mV/sec.

The electrochemical impedance spectra, corresponding to steel corrosion in the absence and in the presence of haematoxylin were recorded in the frequency range of 100 kHz - 10 mHz, with an amplitude of 10 mV.

2.3. UV-Vis spectroscopy

Samples of the 0.1M $NaNO_3$ solutions containing various concentrations of haematoxylin (HX) were used for spectrophotometric analysis, before and after their usage in the corrosion tests of carbon steel. UV-VIS analysis reports were obtained using a UV-VIS spectrophotometer, VARIAN-CARY 50 type.

Procedure: The solutions were placed in the UV-VIS beam and a graph of absorbance *versus* the wavelength was obtained; for each sample analysis, reports were obtained using the soft CARY WIN UV. Alternatively, the solutions were prepared in known concentrations of HX and they were read by the UV-VIS spectrophotometer. Results are graphed to make a calibration curve from which the unknown concentration of can be determined by its absorbance.

2.4. Surfaces morphology

The surface morphologies of the uncorroded and corroded carbon steel, in the absence and in the presence of the inhibitor, were examined by Euromex microscope with Canon camera and included ZoomBrowser - EOS Digital software

3. RESULTS AND DISCUSSION

3.1. Potentiodynamic measurements

The presence of HX in corrosion environment produces changes in both the shape of polarization curves, as well as of their positions, which were shifted in other fields of potential compared with the polarization curve obtained in the absence of HX. From Figure 1, it can be seen that the corrosion potentials are shifted in positive direction, starting with 0.4 mM concentration of HX in aggressive medium. However, polarization curve corresponding to concentration of 0.4 mM, is moved in a higher current region than that obtained for the blank solution. This is associated with an increase in corrosion current indicating that, at the concentration of 0.4 mM, HX accelerates the corrosion process of carbon steel in $NaNO_3$ medium. In the concentration range from 0.6 mM to 1.0 mM, polarization curves are shifted in lower current areas. Both processes, anodic oxidation and cathodic reaction of oxygen reduction, are strongly modified, especially for the last two concentrations of HX, 0.8 mM and 1.0 mM, respectively. Taking these data into account, we may conclude that the corrosion current density decreases starting with the 0.6 mM concentration of HX, reaching the lowest value for the solution containing 1.0 mM HX.
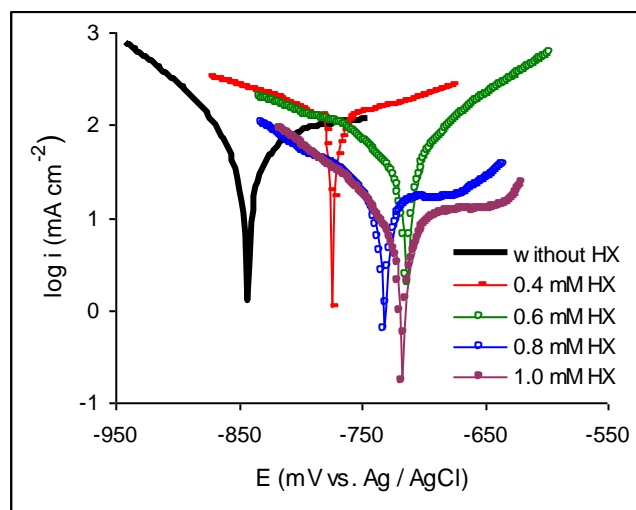

Figure 1. The potentiodynamic curves of carbon steel corroded in 0.1 M $NaNO_3$ solution in the absence and in the presence of different concentrations of HX.

These observations indicate the fact that HX inhibits the corrosion of carbon steel in $NaNO_3$ by blocking the active sites of metal surface by forming a thin organic film [42], which is interposed at the metal/electrolyte interface. It can also be noted that, in the potential range between -710 mV and -660 mV, the current density is constant forming a plateau on the polarization curve of carbon steel corroded in nitrate solution containing 0.8 mM HX, indicating that in this region the metal ionization can be greatly suppressed. At potential values higher than -660 mM, carbon steel becomes active, perhaps with the help of the dissolved oxygen reduction reaction. At lower current density, in the

potential range between -680mV and -630 mV, a similar plateau can be observed on the polarization curve of carbon steel corroded in nitrate solution containing 1.0 mM HX.

The electrochemical parameters such us: corrosion potential (E_{corr}), corrosion current density (i_{corr}), anodic and cathodic Tafel lines (b_a & b_c), as well as inhibition efficiency (*IE*) as a function of HX concentration (C-HX) are presented in Table 1.

The corrosion current density (i_{corr}) was estimated to intersection of anodic and cathodic Tafel lines at corrosion potential, b_a & b_c being estimated for the segments value of 90 mV dec^{-1} using VoltaMaster 4 software. The inhibition efficiency percentage (*IE*) of HX was determined from polarization measurements according to the following equation, Eq. 1 [43-45]:

$$IE = \frac{i^0_{corr} - i_{corr}}{i^0_{corr}} \times 100 \qquad (1)$$

where i^0_{corr} and i_{corr} are the corrosion current densities of carbon steel in 0.1 M NaNO$_3$ solution without and with HX, respectively.

Table 1. Electrochemical parameters and inhibition efficiency obtained from Tafel polarization for carbon steel corroded in 0.1 M NaNO$_3$ solution in the absence and in the presence of different concentration of HX.

C-HX/ mmol L^{-1}	E_{corr}/mV vs.Ag/AgCl	i_{corr}/ μA cm^{-2}	b_a/ mV dec^{-1}	b_c/ mV dec^{-1}	*IE*/ %
0	-843	70.0	262.0	98.0	0
0.4	-774	113.0	218.0	245.0	0
0.6	-712	45.2	114.0	225.0	35.4
0.8	-732	20.2	122.0	118.0	71.1
1.0	-717	11.5	132.0	100.0	83.6

By analysing the data from Table 1 we may conclude that the corrosion current density decreases with the increase in HX concentration starting with 0.6 mM HX in corrosive medium, and consequently, the inhibition efficiency increases, reaching a maximum value of 83.6% at 1.0 mmol L^{-1} HX in 0.1 M NaNO$_3$ solution.

3.2. Action mechanism of HX as corrosion inhibitor

To estimate the most likely mechanism of the carbon steel inhibition by HX, the UV-Vis scans of corrosive media, before and after corrosion processes, were accomplished. In Figure 2, the molecular structure of HX and UV-Vis scans of 0.1 M NaNO$_3$ solution containing 0.4 mM HX and 1.0 mM HX, before and after corrosion, are presented. Note that HX has two adsorption peaks, at 295 nm

and 436 nm, corresponding to the haematoxylin (HX) and its oxidized form, haematein (HT), respectively.

Before corrosion, for both above mentioned concentrations, HT is presented as a flattened shoulder, slightly more nuanced for 1.0 mM HX, indicating that the HT amount in corrosive media is very small. After corrosion, it can be observed that, HX absorbance decreases without altering the wavelength of adsorption maximum, but at the same time, the corresponding peak of HT increases in a considerable manner and a new peak at 558 nm is observed. In our previous studies [46, 47] we showed that, under these experimental conditions, the main product of corrosion is formed by Fe^{3+} species which are similar to those shown by Fe^{3+} oxide/oxyhydroxides. By considering those previously stated, we can say that during potentiodynamic polarization, two simultaneous phenomena appear, as follows: (i) the oxidation of HX to HT (Scheme I); (ii) the formation of a strongly coloured complex of HT with Fe^{3+} ions. In other studies the absorption bands of haematein and haematein complexes were recognized at 445 nm and 556 nm, respectively [48, 49]. Also, this was confirmed by the change of the reaction environment colour during the electrochemical measurements, as follows: light yellow HX solution → red solution (indicating the presence of HT) → violet solution (indicating the presence of the HT complex with Fe^{3+}).
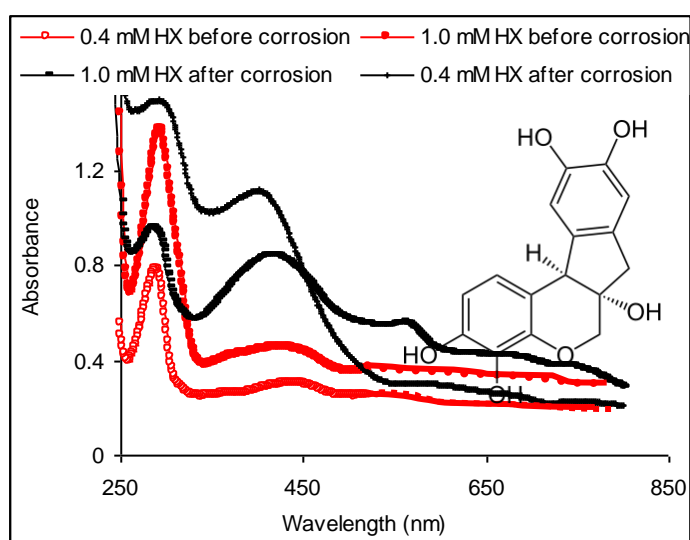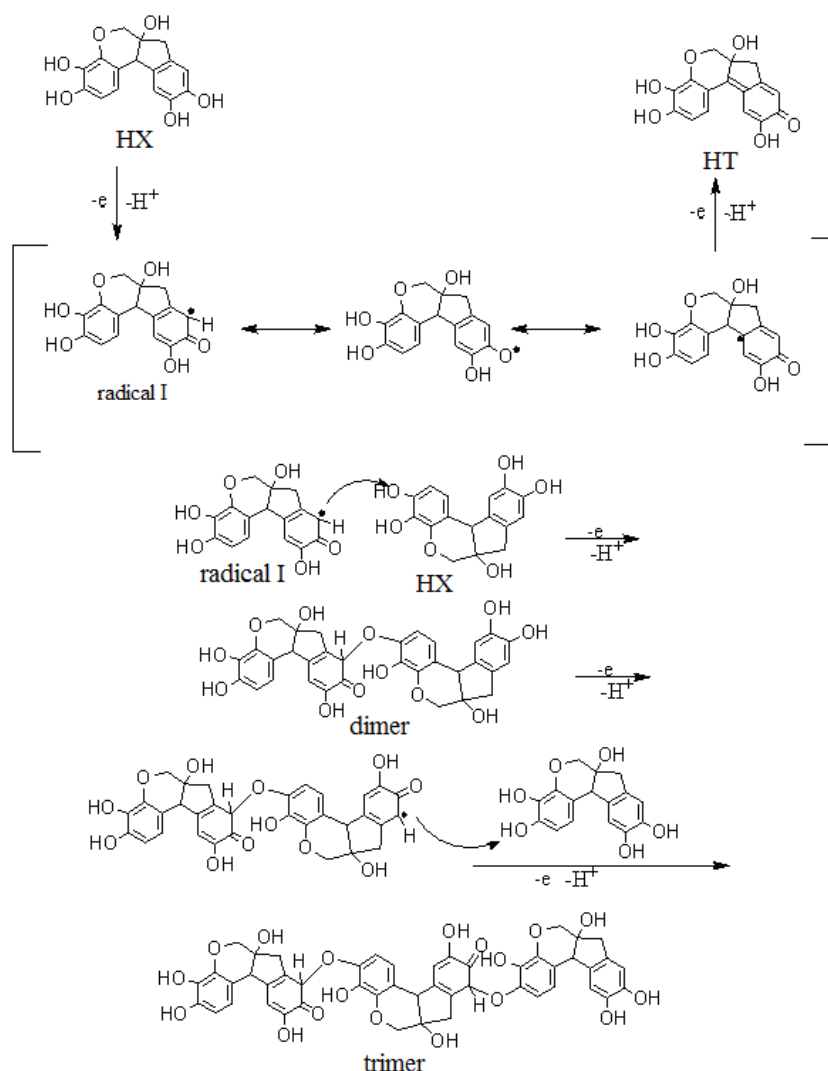

Figure 2. The HX molecular structure and the UV-Vis scans of 0.1 M $NaNO_3$ solution containing 0.4 mM HX and 1.0 mM HX, before and after corrosion tests

Based on these data, we consider that HX acts as inhibitor for carbon steel corrosion in nitrate solution through several mechanisms related to the formation of a thin layer, such as the pure adsorption of HX and HT, as well as complexes formation between HT and iron (III) ions that may provide a good stability of this layer.

Moreover, from Figure 1 it can be observed that the shape of polarization curves obtained for the carbon steel corroded in nitrate solution containing 0.8 mM HX and 1.0 mM HX are very modified compared with the polarization curves obtained for carbon steel corroded in 0.1 M $NaNO_3$ without and

with lower concentrations of HX. This can be explained by occurrence of other phenomena which could change the composition of the thin layer formed on carbon steel surface. Several studies reported that the electropolymerization of HX is also possible under different experimental conditions such as: slightly and neutral pH, 10^{-4} haematoxylin concentration in the potential range of $-0.5 \div 2$ V [50, 52], resulting a poly-haematoxylin film (p-HX) with bioelectrocatalytic activity [50-52]. So, the polymerization of HX should be considered as an additional process contributing to the formation of a protective film on the metal surface.

The proposed mechanisms of HX oxydation and electropolymerization are presented below (Scheme 1).

Scheme 1. Haematein (HT) formation and propagation steps of the electrochemical haematoxylin polymerization mechanism.

From Scheme 1, it can be observed that haematoxylin molecule loses an electron and a proton with formation of an active radical (I), for which resonance structures can be written. In a second

oxidation step of radiacal I, haematein (HT) is formed, this being the stable oxidized form of haematoxylin.

Five different tautomeric forms can be written for hematein, but the values of their free Gibbs energies indicate that the most stable form among them is the HT structure presented in Scheme 1 [53]. Therefore, an oxidation mechanism that would first lead to one of the other four tautomeric forms, that would subsequently tautomerize to the known stable structure of HT, is not excluded either.

The radical (I) may attack a new molecule, forming a haematoxylin dimmer [50, 52]. This dimmer is easily oxidized to a radical-dimer [52]. The radical-dimmer attacks a new molecule of haematoxylin forming a trimer, and this chained process continues until obtaining the stable poly-haematoxylin macromolecule [52].

Taking these data into account, we assume that the action mechanism of HX as inhibitor for carbon steel corrosion in nitrate solution is difficult to assess, but concrete phases of organic film formation could be given, as follows:

- the pure absortion of HX;
- the pure adsorbtion of HT;
- the complexes formation between HT and iron (III) and their adsorption on carbon steel surface;
- electrosynthesis of p-HX film which could insert the HX and HT molecules, different ions, such as: OH^-, NO_3^-, Fe^{3+}, as well as iron compounds and its complexes.

3.3. Electrochemical impedance spectroscopy

Figure 3 shows the Nyquist (Fig.3a) and Bode (Figs.3b and 3c) plots for carbon steel in 0.1 M $NaNO_3$ solution without and with different concentrations of HX; it can be seen that the impedance response of carbon steel in 0.1 M $NaNO_3$ solution shows a significantly change after haematoxylin addition, indicating that, in low frequency range, the carbon steel impedance increases with increasing the inhibitor concentration (Fig.3b) and consequently, the inhibition efficiency increases.

It is also apparent from these plots that Nyquist curves (Fig.3a) are consisted in one capacitive loop and one phase angle maximum in Bode format (Fig.3c). For both plots more pronounced frequency arcs were obtained for the samples which were immersed in 0.1 M $NaNO_3$ solution containing various HX concentrations higher than 0.4 mM.

This behaviour is usually assigned to changes in density and composition of substrate layer [54-57]. It is clear that HX presence produced a higher polarization resistance (R_p) value, which is interpreted in terms of formation of an effective protective layer which is controlled by the process of adsorption and desorption of inhibitor molecule at low frequencies [58, 59], with adsorption predominance. An equivalent circuit is suggested in Figure 3a relating the best fitting of EIS measurements, where R_s is the solution resistance of the bulk electrolyte and C_{coat} is the capacitance of the coating. Typical coating capacitances are on the order of $1\mu F\ cm^{-2}$ [54]. The value can vary based on the thickness of the coating, as well as its dielectric constant [54]. The dielectric constant and thickness can both change over time when exposed to solution, because coating often adsorbs water

[54]. R_{coat} is the resistance of the coating that often has very small pores which contain electrolyte, providing a conduction path of ions through the coating [54]. C_{dl} represents the double layer capacitance of the electrolyte at the metal surface. R_p is the polarization resistance of carbon steel. The impedance parameters derived from EIS measurements and respective fitting results are given in Table 2 and Figure 3, respectively.
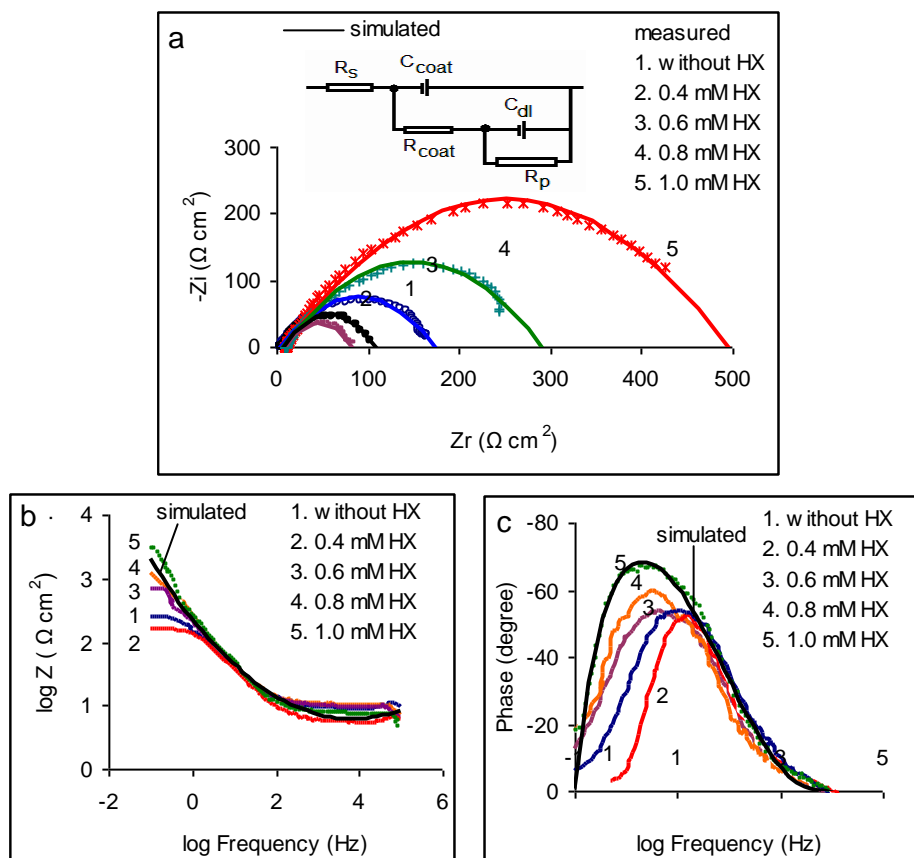

Figure 3. Nyquist plots, equivalent circuit model (a) and Bode plots (b, c) for carbon steel immersed in 0.1 M NaNO₃ blank solution and in 0.1 M NaNO₃ solution containing various concentrations of HX

The fitting results show that R_{coat} and R_p increase with increasing HX concentration, suggesting that the amount of adsorbed species increases, forming a thin organic film. The decrease in C_{coat} and C_{dl} could be attributed to the decrease in local dielectric constant and/or to the increase in thickness of the electrical double layer, signifying that an organic film at the interface of metal/solution was formed [54, 60].

The change in R_{coat}, R_p, C_{coat} and C_{dl} values was caused by the gradual replacement of water molecules by adsorption of the organic film on the metal surface [60]. The R_p was used to calculate the inhibition efficiency from Eq. 2:

$$IE = \left(\frac{R_p - R_p^0}{R_p} \right) \cdot 100 \qquad (2)$$

where R_p and R_p^0 represent the corrosion resistance in the presence and in absence of inhibitor, respectively.

Table 2. Impedance parameters for carbon steel in 0.1 M NaNO$_3$ solution in the absence and in presence of different concentrations of HX, at room temperature

C-HX/ mML^{-1}	R_s/ mΩ cm^2	C_{coat}/ μF cm^{-2}	R_{coat}/ Ω cm^2	C_{dl}/ μF cm^{-2}	R_p/ Ω cm^2	IE/ %
0	38.50	2.5	2.2	1100.0	101.8	0
0.4	11.60	2.2	3.1	819.5	78.9	0
0.6	9.90	1.8	5.3	812.0	172.7	41.1
0.8	6.68	1.6	7.8	714.0	291.8	65.1
1.0	6.20	1.3	9.1	459.0	498.6	79.6

The presence of HX leads to an approx. 80.0% inhibition efficiency, a closely value to those obtained from potentiodynamic curves (Table 2).

3.4. Surface characterization

The microscopic images of carbon steel surfaces before and after potentiodynamic curves obtained in 0.1 M NaNO$_3$ solution without and with various concentrations of HX are presented in Figure 4. The reference sample reveals a characteristic morphology of the carbon steel surface before corrosion process (Fig.4a). The microscopic image from Figure 4b shows that after corrosion, carbon steel surface was coated with large spots which change its texture, but the feature of a film adsorbed on the surface is not nuanced. Moreover, large portions of the surface keep the morphology of the reference sample, indicating that nitrate ions have some protective effect due to their oxidant action.

From Figure 4c to Figure 4f the microscopic images are completely different compared with those presented above, showing a characteristic morphology of protected surfaces. In Figure 4c corrosion spots are equally emphasized, as in Figure 4b, indicating that the formation of anodic areas on which corrosion processes are enhanced, is possible. These confirm the results obtained by electrochemical measurements which showed that 0.4 mM HX in nitrate solution is not the optimal concentration for corrosion inhibition of carbon steel. Figures 4d and 4e show the image of some surfaces covered by a discontinuous layer that could be attributed to an adsorbed organic film. All organic components, such as: HX, HT, p-HX could act as "an incipient rust transformer", favouring the formation of a "superficial closed layer". It is known that the organic components of the rust transformers penetrate the rust and decelerate the rusting process in this way [61]. The surface morphology shown in Figure 4f is different compared with those commented above. The feature of an

organic film, which could be attributed to a polymer layer on carbon steel surface, is more obvious and its uniformity is also evidenced.
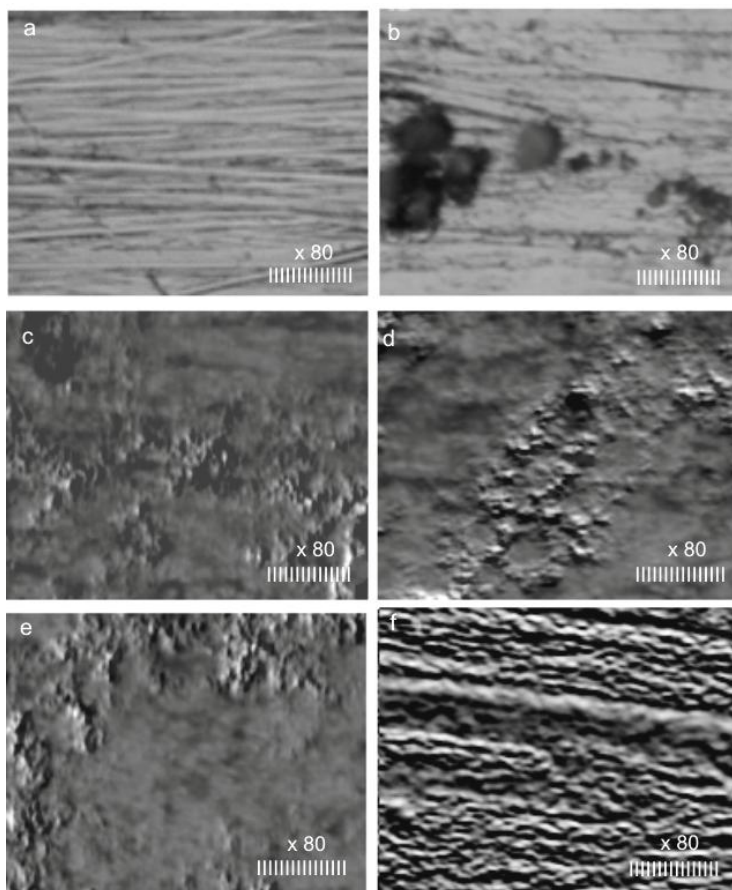

Figure 4. Microscopic images of carbon steel surfaces: a - before corrosion; b- after corrosion in 0.1 M $NaNO_3$ blank solution; c - after corrosion in 0.1 M $NaNO_3$ solution containing 0.4 mM HX; d - after corrosion in 0.1 M $NaNO_3$ solution containing 0.6 mM HX; e - after corrosion in 0.1 M $NaNO_3$ solution containing 0.8 mM HX; f - after corrosion in 0.1 M $NaNO_3$ solution containing 1.0 mM HX

4. CONCLUSIONS

The action mechanism of haematoxylin as inhibitor for carbon steel corrosion in 0.1 M $NaNO_3$ solution was studied using potentiodynamic polarization and electrochemical impedance spectroscopy associated with UV-Vis spectrophotometry.

Both, potentiodynamic polarization and electrochemical impedance spectroscopy measurements showed that HX acts as corrosion inhibitor of carbon steel under the above mentioned laboratory conditions, starting with the concentration value of 0.6 mM.

UV-Vis spectrophotometry confirms the oxidation process of haematoxylin to haematein followed by its Fe^{3+} complexes formation.

A synergic mechanism of corrosion inhibition was proposed, consisting of an organic film formation based on HX and HT pure adsorbtion supplemented by HT complexes with Fe^{3+} ions occurrence, and HX electropolymerization.

References

1. D. Wahyuningrum, S. Achmad, Y.M. Syah, Buchari, B. Bundjali and B. Ariwahjoedi, *Int. J. Electrochem. Sci.*, 3 (2008) 154.
2. G.R.H. Florence, A.N. Anthony, J.W. Sahayaraj, A.J. Amalraj and S. Rajendran, *Ind. J. Chem. Technol.*, 12 (2005) 472.
3. A. Samide and B. Tutunaru, *J. Environ. Sci. Health, Part A*, 46 (2011) 1713.
4. P.K. Gogoi and B. Barhai, *Int. J. Electrochem. Sci.*, 6 (2011) 136.
5. J. Hmimou, A. Rochdi, R. Touir, M. Ebn Touhami, E.H. Rifi, A. El Hallaoui, A. Anouar and D. Chebab, *J. Mater. Environ. Sci.*, 3 (2012) 543.
6. A. Samide, I. Bibicu, M.S. Rogalski and M. Preda, *Corros. Sci.,* 47 (2005) 1119.
7. A. Samide and I. Bibicu, *Surf. Interface Anal.,* 40 (2008) 944.
8. A. Samide, I. Bibicu, M. Agiu and M. Preda, *Mater. Lett.,* 62 (2008) 320.
9. A. Samide, I. Bibicu and E. Turcanu, *Chem. Eng. Commun.,* 196 (2009) 1008.
10. A. Samide, B. Tutunaru, Catalin Negrila, I. Prunaru, *Spectroscop. Lett.*, 45 (2012) 55.
11. A. Samide, B. Tutunaru, *Chem. Biochem. Eng. Q.*, 25 (2011) 299.
12. S.S.A. Rehim, O.A. Hazzazi, M.A. Amin and K.F. Khaled, *Corros. Sci.*, 50 (2008) 2258.
13. M. Mobin, M. Parveen and M.A. Khan, *Recent Res. Sci. Technol.*, 3 (2011) 40.
14. H.M. El-Lateef, L.I. Aliyeva, V.M. Abbasov and T.I. Ismayilov, *Adv. Appl. Sci. Res.*, 3 (2012) 1185.
15. A.A. Maghraby and T.Y. Soror, *Adv. Appl. Sci. Res.*, 1 (2010) 156.
16. M. Sharma, J. Chawla and G. Singh, *Indian J. Chem. Technol.*, 16 (2009) 339.
17. F.A. Ansari and M.A. Quraishi, *Portugaliae Electrochim. Acta*, 28 (2010) 321.
18. Q.B. Zhang and Y.X. Hua, *Electrochim. Acta*, 54 (2009) 1881.
19. N.V. Likhanova, O. Olivares-Xometl, D. Guzman-Lucero, M.A. Dominguez-Aguilar, N. Nava, M. Corrales-Luna and M.C. Mendoza, *Internat. J. Electrochem. Sci.*, 6 (2011) 4514.
20. M.A.M. Ibrahim, M. Messali, Z. Moussa, A.Y. Alzahrani, S.N. Alamry and B. Hammouti, *Portugaliae Electrochim. Acta*, 29 (2011) 375.
21. R.S.A. El-Hameed, *Adv. Appl. Sci. Res.*, 2 (2011) 483.
22. N. Manimaran, S. Rajendran, M. Manivannan and S. John Mary, *Res. J. Chem. Sci.*, 2 (2012) 52.
23. S.A. Umoren, U.M. Eduok and E.E. Oguzie, *Portugaliae Electrochim. Acta*, 26 (2008) 533.
24. A.K. Dubey and G Singh, *Portugaliae Electrochim. Acta*, 25 (2007) 221.
25. S. Merah, L. Larabi, O. Benali and Y. Harek, *Pigm. Resin Technol.*, 37 (2008) 291.
26. O. Benali, L. Larabi, S. Merah and Y. Harek, *J. Mater. Environ. Sci.*, 2 (2011) 39.
27. H. Ashassi-Sorkhabi and D. Seifzadeh, *J. Appl. Electrochem.*, 38 (2008) 1545.
28. M. Abdeli, N.P. Ahmadi and R.A. Khosroshahi, *J. Sol. State. Electrochem.*, 14 (2010) 1317.
29. E.E. Ebenso, H. Alemu, S.A. Umoren and I.B. Obot, *Int. J. Electrochem. Sci.*, 3 (2008) 1325.
30. A.I. Onen, O.N. Maitera, J. Joseph and E.E. Ebenso, *Int. J. Electrochem. Sci.*, 46 (2011) 2884.
31. H. Ashassi-Sorkhabi, B. Masoumi, P. Ejbari and E. Asghari, *J. Appl. Electrochem.*, 39 (2009) 1497.
32. H. Ashassi-Sorkhabi, E. Asghari and P. Ejbari, *Acta Chim. Slov.*, 58 (2011) 270.
33. E.E. Ebenso, T. Arslan, F. Kandemirli, I. Love, C. Ogretir, M. Saracoglu and S.A. Umoren, *Internat. J. Quant. Chem.*, 110 (2010) 2614.
34. N.O. Eddy, S.A. Odoemelam and P. Ekwumemgbo, *Sci. Res. Essay*, 4 (2009) 033.
35. S.U. Ofoegbu and P.U. Ofoegbu, *J. Eng. Appl. Sci.*, 7 (2012) 272.

36. S.H. Kumar and S. Karthikeyan, *J. Mater. Environ. Sci.*, 3 (2012) 925.
37. A. Samide, *J. Environ. Sci. Health, Part A*, 48 (2013) 159.
38. M. Znini, G. Cristofari, L. Majidi, A. Ansari, A. Bouyanzer, J. Paolini, J. Costa and B. Hammouti, *Int. J. Electrochem. Sci.*, 7 (2012) 3959.
39. K.P. Vinod Kumar, M. Sankara Narayanan Pillai and G. Rexin Thusnavis, *J. Mater. Environ. Sci.*, 1 (2010) 119.
40. A.P.I. Popoola, M. Abdulwahab and O.S.I. Fayomi, *Int. J. Electrochem. Sci.*, 7 (2012) 5805 .
41. V. Sribharathy, S. Rajendran and J. Sathiyabama, *Chem. Sci. Trans.*, 2 (2013) 315.
42. B. Zerga, A. Attayibat, M. Sfaira, M. Taleb, B. Hammouti, M. Ebn Touhami, S. Radi, Z. Rais, *J. Appl. Electrochem.,* 40 (2010) 1575.
43. Y. H. Ahmad, A. S. Mogoda, A. G. Gadallh, *Int. J. Electrochem. Sci.,* 7 (2012) 4929.
44. El-Mehdi, B. Mernari, M. Traisnael, F. Bentiss, M. Lagrenee, *Mater. Chem. Phys.*, 77 (2002) 489.
45. A. Moanta, A. Samide, C. Ionescu, B. Tutunaru, A. Dobritescu, A. Fruchier, V. Barragan-Montero, *Int. J. Electrochem. Sci.,* 8 (2013) 780.
46. A. Samide, I. Bibicu, M. Rogalsky, M. Preda, *J. Radioanal. Nucl. Chem.*, 261 (2004) 593.
47. B. Tutunaru, A. Samide, C. Negrila, *J. Therm. Anal. Calorim.*, 2012: DOI 10.1007/s10973-011-2187-0.
48. Ch. Bettinger, H.W. Zimmermann, *Histochemistry*, 96 (1991) 215.
49. Ch. Bettinger, H.W. Zimmermann, *Histochemistry*, 95 (1991) 275.
50. D. G. Dilgin, D. Gligor, H. I. Gokcl, Z. Dursun, Y. Dilgin, *Biosens. Bioelectron.,* 26 (2010) 411.
51. H. R. Zare, N. Nasirizadeh, *Electrochim. Acta*, 56 (2011) 3920.
52. B. Tutunaru, A. Samide, G. Bratulescu, *J. Appl. Polym. Sci.*, submitted.
53. H. Beiginejad, D. Nematollahi, M. Bayat, *J. Electroanal. Chem.*, 681 (2012) 76.
54. W. Stephen Tait, *An Introduction to Electrochemical Corrosion Testing for Practicing Engineers and Scientists,* Pair O Docs Publications (1994).
55. K. Juttner, *Electrochim. Acta*, 35 (1990) 1501.
56. T. Pajkossy, *J. Electroanal. Chem.*, 364 (1994) 111.
57. W.R. Fawcett, Z. Kovacova, A. Motheo, C. Foss. *J. Electrochem. Soc.*, 326 (1992) 91.
58. E. Mcafferty, N. Hackerman, *J. Electrochem. Soc.*, 119 (1972) 146.
59. R. Solmas, G. Kardas, B. Yazicl, M. Erbil, *Colloids and surfaces A: Physicochem. Eng. Aspects*, 312 (2008) 7.
60. S. Muralidharan, K. L. N. Phani, S. Pitchumani, S. Ravichandran, and S. V. K. Iyer, *J.Electrochem. Soc.*, 142 (1995) 1478.
61. Meisel W, Gutlich P. *Werkst. Korros.*, 32 (1981) 296.